Microchimica Acta
https://doi.org/10.1007/s00604-019-3226-y

ORIGINAL PAPER

Simultaneous fluorometric determination of the DNAs of *Salmonella enterica*, *Listeria monocytogenes* and *Vibrio parahemolyticus* by using an ultrathin metal-organic framework (type Cu-TCPP)

Qiming Qiu[1] · Huayun Chen[1] · Shengna Ying[1] · Sumaira Sharif[1] · Zhiheng You[1] · Yixian Wang[1] · Yibin Ying[1,2]

Received: 26 October 2018 / Accepted: 2 January 2019

Abstract
Ultrathin (<10 nm) nanosheets of a metal-organic framework (MOF-NSs) were prepared in high-yield and scalable production by a surfactant-assisted one-step method. The MOF-NSs possess distinguished affinity for ssDNA but not for dsDNA. This causes the fluorescence of the labeled DNA to be quenched. On binding to the target DNA (shown here for *Salmonella enterica*, *Listeria monocytogenes* and *Vibrio parahemolyticus*), the labeled duplex is released and the fluorescence of the label is restored. The labels Texas Red, Cy3 and FAM were used and give red, red or green fluorescence depending on the kind of pathogen. The detection limits are 28 pM, 35 pM and 15 pM for the gene segments of *Salmonella enterica*, *Listeria monocytogenes* and *Vibrio parahemolyticus*, respectively.

Keywords Two dimensional nanomaterials · Surfactant-assisted synthesis · FRET · Pathogens · Fluorescence sensor · Multiplex detection

Introduction

The sensitive, specific, rapid, and cost-effective detection of nucleic acids has found widespread applications in clinical disease diagnostics, gene analysis, industrial and environment monitoring, and food safety detection [1–3]. Great efforts have been contributed to develop numerous electrochemical and optical approaches for the detection of nucleic acids [4]. The introduction of simple synthesis strategies for fluorescently labeled nucleic acids has significantly promoted the research and application of nucleic acid probes. In the past decade, the homogenous fluorescence assays based on Förster resonance energy transfer (FRET) or fluorescence quenching mechanism between fluorescent probes and nanomaterials have been widely developed [5, 6]. So far, many two-dimensional (2D) nanomaterials, such as graphene [7, 8], nanographite [9], transition metal dichalcogenides (TMDs) [10], metal oxides [11], boron nitride (BN) [12], and carbon nitride (CN) [13], have been successfully synthesized. Because of their effective adsorption and excellent quenching efficiency towards dye-labeled ssDNA, these 2D nanomaterials are used to fabricate fluorescent biosensors. For instance, Lu et al. reported a dye-labeled ssDNA probe that is absorbed on graphene oxide surface. This leads to the quenching of the fluorescence of the probe [14]. When the probe bound to the target, the fluorescence was retained via releasing the probe from GO surface. Zhu et al. reported that molybdenum disulfide nanosheets were used for fabricating fluorescent nanosensors for detecting DNA and adenosine showing excellent sensitivity and short assay time [15]. The success fabrication of these fluorescent sensors with high sensing performance depends on the ratio of signal-to-noise. Ideally, the nanomaterials have high adsorption and quenching ability towards to dye-labeled ssDNA and a large enhance in the fluorescence signal towards to dsDNA. Therefore, it is of great importance to further explore novel materials with convenient structural design and tunability to possess excellent adsorption and quenching ability towards to dye-labeled ssDNA.

Electronic supplementary material The online version of this article (https://doi.org/10.1007/s00604-019-3226-y) contains supplementary material, which is available to authorized users.

✉ Yixian Wang
yixianwang@zju.edu.cn

[1] School of Biosystems Engineering and Food Science, Zhejiang University, Hangzhou 310058, People's Republic of China

[2] Zhejiang A&F University, Hangzhou 310058, People's Republic of China

Published online: 10 January 2019

Metal organic frameworks (MOFs) are periodic porous crystalline formed by organic ligands coordinated with metal atom nodes. MOFs have advantages of well-defined chemical structure, convenient structural design and tunability, and readily accessible active sites [16, 17]. Due to the aboved features, MOFs have been intensively used in sensing applications including fluorescent [18, 19], electrochemical [20, 21], electrochemiluinescent [22, 23], and colorimetric sensors [24]. For example, a MOF, *N*,*N*′-bis(2-hydroxyethyl)dithiooxamidato copper(II) [Cu(H_2dtoa)], was demonstrated that it can absorb ssDNA probe and quench fluorescence of FAM-labeled ssDNA probe via photoinduced electron transfer (PET) [25]. The MOF was used to develop a sensitive fluorescent biosensor for detecting target DNA with a linear range of 10–100 nM. However, the traditional MOFs are bulk crystalline. The bulk MOFs still suffer from poor dispersion in solution and low accessible active sites, which hinder their applications in biosensors.

As a new family member of 2D nanomaterials, MOF nanosheets are an effective material for fabricating the fluorescence platform. Because MOF nanosheets possess some excellent features including high surface area and numerous accessible active sites on sheet surface, which exhibit an effective fluorescence quench property and reduce the noise of the sensor to improve sensitivity. The strong adsorption property of MOF nanosheets also reduces the response time. MOF nanosheets were successfully prepared using two strategies, i.e., bottom-up and top-down methods. The MOF nanosheets can be exfoliated from bulk layered MOFs using top-down methods because of the weak interlayer interaction [26–28]. However, this method is difficult to prepare MOF nanosheets with uniformity and high yield, which is limit for the various applications. A surfactant-assisted synthetic method as one kind of bottom-up method, has been reported for the preparation of uniform and high-yield MOF nanosheets [29–31]. Such a method may open the door for exploring 2D MOF nanomaterials in various application fields [30]. Herein, we developed a MOF nanosheet-based fluorescence biosensor for rapid, sensitive, and multiplex detection of pathogenic genes, including invA gene of *Salmonella enterica* (*S. enterica*), prfA gene of *Listeria monocytogenes* (*L. monocytogenes*), and toxR gene of *Vibrio parahemolyticus* (*V. parahemolyticus*). A surfactant-assisted method was used to prepare the MOF nanosheets (named as Cu-TCPP) that constructed by copper ion (as metal node) and tetrakis(4-carboxyphenyl)porphyrin (TCPP, as organic ligand). Results demonstrate that the MOF nanosheets can effectively quench the fluorescence of organic dyes, including Texas red (excitation/emission at 589 nm/616 nm), Cy3 (excitation/emission at 540 nm/562 nm), and FAM (excitation/emission at 490 nm/520 nm). Furthermore, a fluorescent biosensor using Cu-TCPP nanosheets was fabricated for multiplex pathogenic genes detection with high sensitivity and short detection time.

Experimental

Chemicals

Copper nitrate trihydrate ($Cu(NO_3)_2{\cdot}3H_2O$), polyvinylpyrrolidone (PVP, average wt 40, 000), and ethanol were purchased from Sigma-Aldrich (St. Louis, MO, https://www.sigmaaldrich.com/china-mainland.html). Tetrakis(4-carboxyphenyl)porphyrin (TCPP, 97%) was obtained from Tokyo Chemical Industry (Shanghai, China, https://www.tcichemicals.com/zh/cn/index.html). *N*,*N*-Dimethylformamide (DMF, 99.8%) and trifluoroacetic acid (CF_3COOH, 99%) were purchased from Alfa Aesar (Heysham, United Kingdom, https://www.alfa.com/zh-cn/). The DNA sequences were synthesized from Sangon Biotech. Co., Ltd. (Shanghai, China, https://www.sangon.com/). The sequences of all DNA are summarized in Table S1.

Preparation of the copper(II) tetrakis(4-carboxyphenyl)porphyrin (Cu-TCPP) nanosheets

$Cu(NO_3)_2{\cdot}3H_2O$ (3.6 mg, 0.015 mmol), trifluoroacetic acid (1.0 M, 10 μL), and PVP (10.0 mg) were added in 12 mL of the mixed liquor (V_{DMF}:$V_{ethanol}$ = 3:1) to obtain mother liquid A. TCPP (4.0 mg, 0.005 mmol) was added in 4 mL of the mixed liquor B (V_{DMF}:$V_{ethanol}$ = 3:1) to prepare mother liquid B. After that, the mother liquid A was added dropwise into the mother liquid B under stirring and sonicated for 10 min. The mixture was heated at 80 °C for 3 h. The resulting products were centrifuged at 8000 r.p.m. for 10 min and re-dispersed in ethanol for characterization.

Characterizations

Prior to the transmission electron microscopy (TEM), scanning electron microscopy (SEM), and atomic force microscopy (AFM) characterization, the Cu-TCPP nanosheets were dropped onto Si/SiO_2, holey carbon-coated carbon support copper grids, and piranha-cleaned Si/SiO_2, respectively. TEM was operated at an acceleration voltage of 200 kV (JEOL-JEM-1200EX). SEM image was obtained via a field emission scanning electron microscope (SEM, Hitachi-SU8010). AFM (Dimension Icon, Bruker) was used to characterize the MOF nanosheets in tapping mode in air. Fluorescence spectra were recorded with a BioTek ELIASA (Synergy Neo2).

DNA detection

Firstly, 10 μL of probe (0.4 μM of P1, or 0.24 μM of P2, or 0.1 μM of P3) was hybridized with 10 μL of target DNA (T,

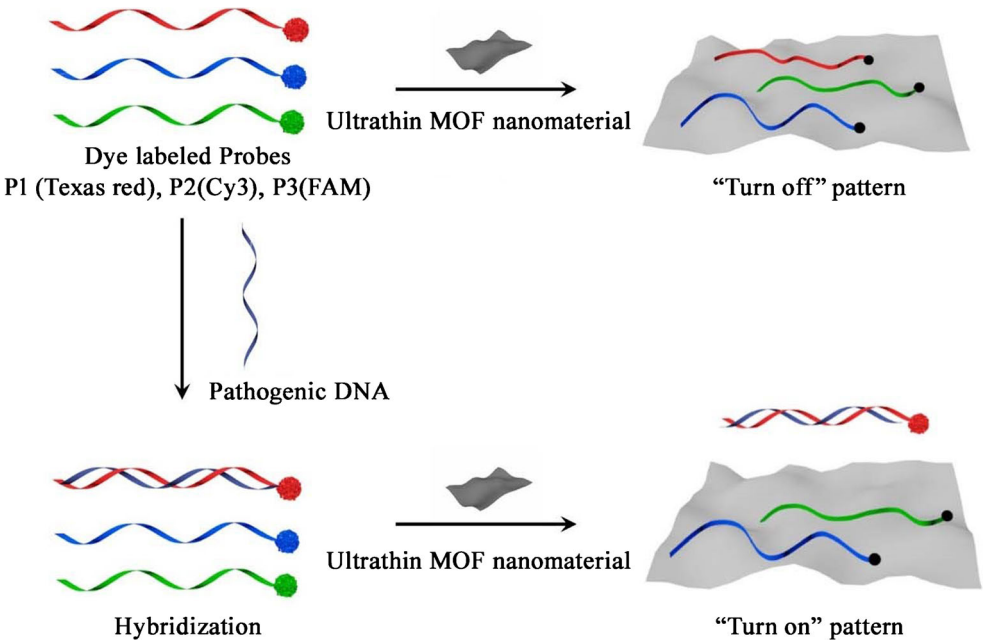

Fig. 1 Schematic illustration of the fluorescent biosensor for multiplex detection of DNAs based on Cu-TCPP nanosheets

0–1.5 μM) in 170 μL of phosphate buffer (pH 7.4, 0.01 M) and incubated for 60 min. Then, 10 μL of Cu-TCPP nanosheet solution at final concentration of 43 μg mL^{-1} was added into the aforementioned solution and the mixture was incubated for 20 min. The fluorescence spectra of the mixture were recorded. To get the optimal concentration of Cu-TCPP nanosheets, the fluorescence spectra of P1 (20 nM) and P1/T1 (P1, 20 nM; T1, 20 nM) were studied with Cu-TCPP nanosheets at different final concentration (8.6, 17.2, 25.8, 34.4, 43, 51.6, and 60.2 μg mL^{-1}). In multicolor DNA assays, 10 μL of P1

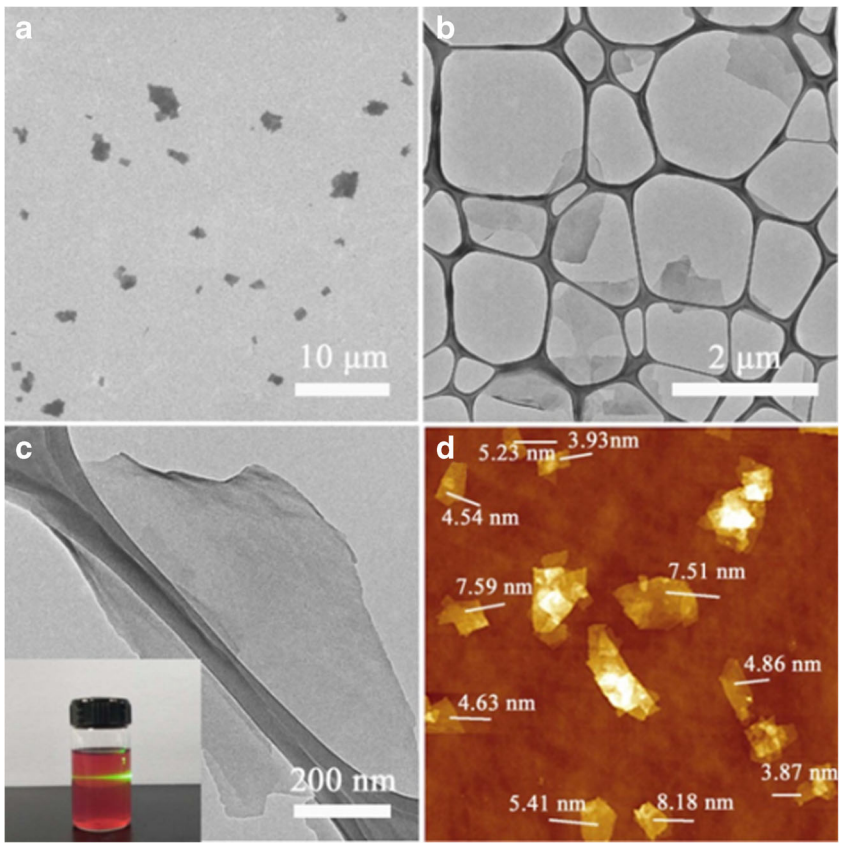

Fig. 2 Characterization of Cu-TCPP nanosheets. **a** Scanning electron microscopy image and **b** low-magnification transmission electron microscopy image of Cu-TCPP MOF nanosheets. **c** Transmission electron microscopy image of a typical Cu-TCPP MOF nanosheet. Inset in (**b**): Photograph of Cu-TCPP MOF nanosheet solution. **d** Atomic force microscopy height image of Cu-TCPP MOF nanosheets

(0.13 μM), 10 μL of P2 (0.08 μM), and 10 μL of P3 (0.03 μM) were mixed in a solution. All the following conditions were similar with those in the single target detection.

Results and discussion

The sensing principle for multiplex determination of DNAs is shown in Fig. 1. Three DNA probes (P1, P2, and P3) targeting three types of pathogen genes (segments of *S. enterica*, *L. monocytogenes*, and *V. parahemolyticus* genes) were employed, which were labeled with dyes (Texas red, Cy3, and FAM), respectively. The three dyes were individually excited at 589 nm (Texas red), 540 nm (Cy3), and 490 nm (FAM), emitting at 616 nm, 562 nm, and 520 nm, respectively, which avoided dye-to-dye energy transfer. These three dye-labeled ssDNA probes (P1, P2, and P3) can easily adsorb on the large surface of MOF nanosheets due to π-electron system of TCPP ligand, resulting in fluorescence quenching of these dye-labeled ssDNA by FRET. When the specific target is added into the three probe mixtures (P1, P2, and P3), the probe hybridizes with its complementary target DNA to form dsDNA. The formed dsDNA detaches from MOF nanosheets due to the weak physical adsorption between the 2D MOF and dsDNA. Based on this principle, the 2D MOF-based sensor is expected to be used for the multiplex detection of DNAs.

The ultrathin Cu-TCPP MOF was prepared by a surfactant-assisted method. The polyvinylpyrrolidone (PVP) as one kind of surfactant molecules is critical to control growth of MOF crystals via selectively attached on the surface of MOFs. Eventually Cu-TCPP nanosheets are synthesized due to the anisotropic growth of MOFs. In the Cu-TCPP MOF nanosheets, the TCPP ligands are metallated by Cu^{2+} ions. The 2D layered sheet is formed by one TCPP ligand coordinated with four Cu paddlewheel metal nodes ($Cu_2(COO)_4$). In the interlayer structure, the Cu atoms in the $Cu_2(COO)_4$ are aligned with the Cu atoms in the centers of TCPP, following an AB packing pattern. The SEM, TEM, and AFM were applied for the characterization of ultrathin Cu-TCPP MOF nanosheets (Fig. 2). As shown in Fig. 2a (SEM image) and Fig. 2b (TEM image), the Cu-TCPP MOF appears the sheet-like structure with the size in the range of hundreds of nanometers to several micrometers. Furthermore, a typical Cu-TCPP nanosheet with size of ~1 μm is observed in Fig. 2c. A typical Tyndall effect can be seen after a green laser goes through the MOF suspension (inset in Fig. 2c), which indicates the colloidal structure of the synthesized MOF nanosheets. As shown in the AFM image (Fig. 2d), the thickness of the Cu-TCPP nanosheets is less than 10 nm.

The fluorescence quenching ability to dye-labeled ssDNA and affinity difference towards ssDNA and dsDNA of Cu-TCPP nanosheets was first investigated. As shown in Fig. 3a, Texas red dye-labeled P1 shows a large fluorescence emission at 616 nm wavelength when the tested solution contains no Cu-TCPP nanosheets. After incubation with Cu-TCPP, the fluorescence of P1 obviously decreased (black curve in Fig. 3a). To get the optimal concentration of the added Cu-TCPP nanosheet, different concentrations of Cu-TCPP were incubated with P1 or P1/T1. The fluorescence peaks of P1 and P1/T1 decrease with the increasing of Cu-TCPP concentrations (Fig. S1a). The fluorescence intensity ratio ($F_{P1/T1}/F_{P1}$) increases as the increasing of Cu-TCPP concentration, and reaches the largest value at 43 μg mL^{-1} (Fig. S1b). At the optimal concentration of Cu-TCPP nanosheets (43 μg mL^{-1}), the quenching efficiency (QE) of MOF nanosheets on the fluorescence of Texas red is 97%. Furthermore, after incubation of 20 min, the fluorescence intensity reaches steady value (Fig. 3b). The result indicates that the strong adsorption between ssDNA and Cu-TCPP nanosheets, and the effective fluorescence quenching efficiency of MOF nanosheets. When the P1 solution was added with target DNA (T1) in a ratio of 1:1 (P1:T1), P1 interacted with T1 to form P1/T1 dsDNA, and consequently the fluorescence intensity of P1/T1 retained in presence of Cu-TCPP nanosheets (red curve in Fig. 3a and b). Such a phenomenon indicates the weaker affinity of Cu-TCPP nanosheets to dsDNA than ssDNA. The

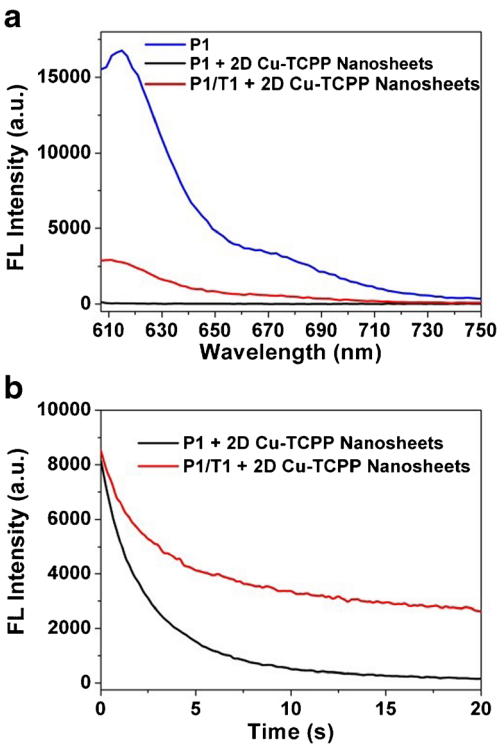

Fig. 3 **a** Fluorescence spectra of P1 under different conditions: P1 (blue curve), P1/T1 + Cu-TCPP nanosheets (red curve), P1 + Cu-TCPP nanosheets (black curve). **b** The fluorescence quenching curves for P1 (black curve) and P1/T1 (red curve) in the presence of Cu-TCPP nanosheets (43 μg mL^{-1}). The concentration of P1 and T1 was 20 nM and 20 nM, respectively. The excitation and emission wavelengths are 589 and 616 nm, respectively

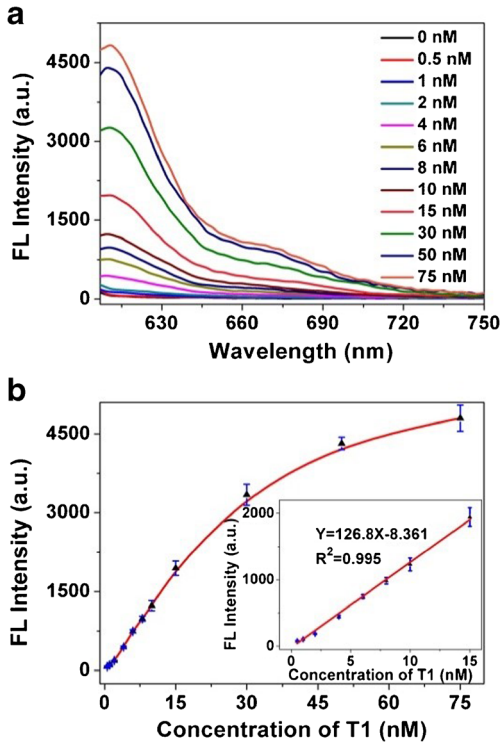

Fig. 4 **a** Fluorescence spectra of P1 (20 nM) in the presence of different concentrations of T1 (0, 0.5, 1, 2, 4, 6, 8, 10, 15, 30, 50, 75 nM) with addition of Cu-TCPP nanosheets (43 μg mL^{-1}). **b** Calibration plot of DNA detection. Inset: The linear plot of fluorescence peak intensity of P1 vs the concentration of T1 with addition of Cu-TCPP nanosheets (43 μg mL^{-1}). The excitation and emission wavelengths are 589 and 616 nm, respectively

reason can be ascribed to the shield of phosphate backbones on the nucleotide bases in the dsDNA and the rigid duplex structure of dsDNA weakens the π-interaction between Cu-TCPP nanosheets and dsDNA. The different affinities of Cu-TCPP nanosheets toward dsDNA and ssDNA suggest the feasibility of Cu-TCPP nanosheets application in the homogeneous detection of DNA.

To further investigate the quenching mechanism between Cu-TCPP nanosheets and Texas red dye-labeled ssDNA, the fluorescence intensity of Texas red-labeled ssDNA at 616 nm was measured after incubation with different concentrations of Cu-TCPP. In common, there are two kinds of fluorescence quenching modes including dynamic quenching and static quenching. The dynamic quenching follows Stern-Volmer (SV) equation, while the static quenching can be described by Lineweaver-Burk (LB) equation [32, 33]. With increasing the concentrations of Cu-TCPP nanosheets, the change of fluorescence intensity of P1 exhibits a good linear correlation (R^2 = 0.967) according to the LB equation (Fig. S2a), while can not follow SV equation (Fig. S2b). Besides, after the addition of MOFs nanosheets, the adsorption peak of Texas red-labeled ssDNA displays an obviously blue shift for 8 nm (Fig. S2c). All the results indicate that the fluorescence quenching of Cu-TCPP towards Texas red-labeled ssDNA follow a static quenching process [32, 33] and the quenching constant of Cu-TCPP is 16.87 μg mL^{-1} by calculation with LB equation.

Based on the aforementioned results, the Cu-TCPP nanosheets serve as an advanced nanoquencher of fluorescent biosensor for quantitatively determination of pathogenic DNA. T1 with different concentrations from 0 to 75 nM were hybridized with P1 (20 nM) for 1 h and then incubated with MOF nanosheets to determine the sensitivity of MOF nanosheet-based biosensing platform. The fluorescence intensity increases with the concentration of T1 increases (Fig. 4a). According to the calibration plot (Fig. 4b), this florescent biosensor shows a linear range from 0.5 to 15 nM, with a detection limit (LOD) of 28 pM (LOD = 3σ/S, σ is the standard deviation of the background signal and S represents the slope of the calibration plot). For Cy3-labeled probe (P2) and FAM-labeled probe (P3), linear relationship in the range of 0.1–12 nM and 0.1–9 nM are obtained, detection limits of 35 pM and 15 pM are achieved, respectively (Fig. S3 and S4). Compared with other nanomaterial-based optical methods for detecting pathogenic DNAs (Table S2), the MOF nanosheet-based fluorescent sensor has a lower detection limit and comparable assay time, demonstrating the excellent performance for detecting trace pathogenic DNAs.

To evaluate the specificity of Cu-TCPP nanosheet-based biosensing platform, the complementary target (T1, T2, and

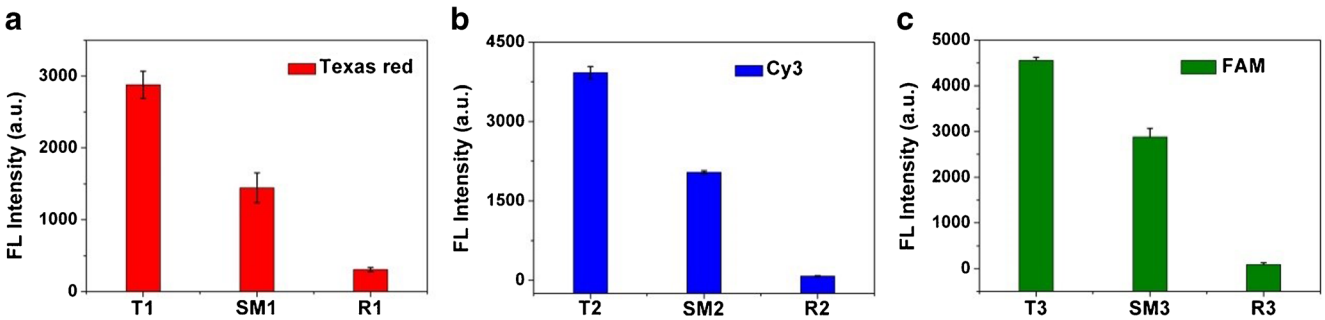

Fig. 5 Selectivity of (**a**) P1, (**b**) P2, and (**c**) P3 by using the complementary target DNA (T1, T2, and T3), single-base mismatch DNA (SM1, SM2, and SM3), and random DNA (R1, R2, and R3). The concentration of P1, T1, SM1, and R1 was all 20 nM. The concentration of P2, T2, SM2, and R2 was all 12 nM. The concentration of P3, T3, SM3, and R3 was all 5 nM. The excitation/emission wavelengths for P1, P2, and P3 are 589/616 nm, 540/562 nm, and 490/520 nm, respectively

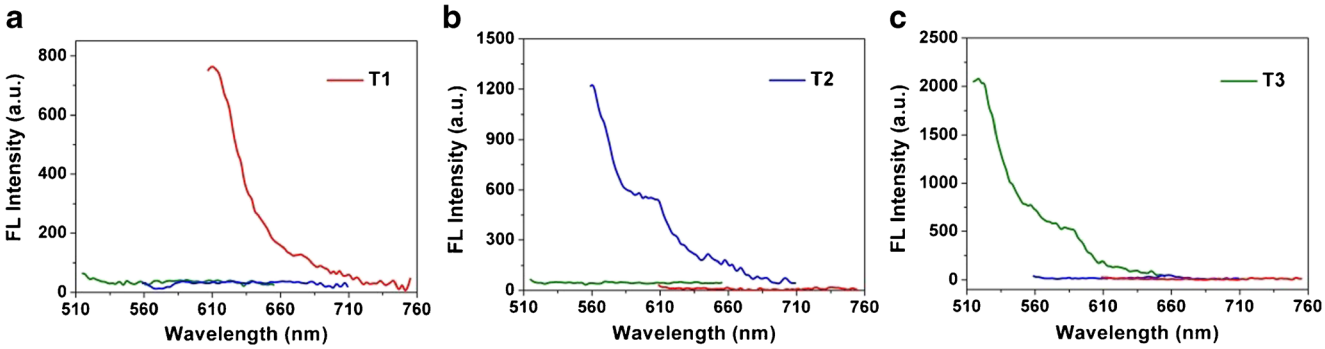

Fig. 6 Fluorescence spectra for multiplex fluorescent DNA detection. Three probes (6.5 nM P1, 4 nM P2, and 1.5 nM P3) were mixed in the presence of different targets (**a**) T1, (**b**) T2, and (**c**) T3. The concentration of T1, T2, and T3 was 6.5, 4, and 1.5 nM, respectively

T3), single-base mismatch DNA (SM1, SM2, SM3 for P1, P2, P3, respectively), and random DNA (R1, R2, R3 for P1, P2, P3, respectively) were investigated. As shown in Fig. 5, the fluorescence signal for the complementary target is approximately two times higher than that for single-base mismatch DNA. The fluorescence of random DNA shows negligible fluorescence response. This demonstrates the MOF nanosheet-based fluorescent nanosensor exhibits satisfactory specificity, which offers great opportunity for multiplex detection of pathogenic DNAs.

It is of great importance to sensing various pathogens due to their serious harm to human health and caused economic loss [34, 35]. The Cu-TCPP nanosheet-based biosensing platform was therefore applied to simultaneously detect various pathogenic genes (T1, T2, or T3) using the mixture of different dyes labeled-probes (P1, P2, and P3). The addition of T1 generates specific emission of P1 at 616 nm wavelength (Fig. 6a). Similarly, T2 results in emissions of P2 at 562 nm wavelength (Fig. 6b) and T3 leads to the emission of P3 at 520 nm wavelength (Fig. 6c). These results suggest that the applicability of Cu-TCPP nanosheet-based fluorescent biosensor towards multiplex DNA detection.

Conclusions

In summary, we prepared ultrathin MOF nanosheets in high-yield and large-scale in solution by a surfactant-assisted method. The MOF nanosheets exhibit different affinities toward dsDNA and ssDNA, and high quenching abilities towards several fluorescent molecules. Such properties make Cu-TCPP nanosheets as an advanced biosensing platform for quantitatively fluorescent detection of pathogenic DNA, showing excellent sensitivity and selectivity with detection limit in pM level. In addition, MOF nanosheet-based nanosensor was successfully applied for multiplex detection of pathogenic genes. This work paves a new way by implementing of 2D MOF nanomaterials into florescent biosensing devices for the development of rapid and robust multiplex detection method of biological molecules.

Acknowledgements The authors are grateful for financial support from National Key Research and Development Program of China (No. 2017YFC1601700) and National Natural Science Foundation of China (No. 31401568).

Compliance with ethical standards The author declare that they have no competing interests.

References

1. Du Y, Li BL, Wang E (2013) "fitting" makes "sensing" simple: label-free detection strategies based on nucleic acid aptamers. Acc Chem Res 46:203–213
2. Jung C, Ellington AD (2014) Diagnostic applications applications of nucleic acid circuits. Acc Chem Res 47:1825–1835
3. Zhao YX, Chen F, Li Q, Wang LH, Fan CH (2015) Isothermal amplification of nucleic acids. Chem Rev 115:12491–12545
4. Kong C, Wang Y, Fodjo EK, Yang GX, Han F, Shen XS (2017) Loop-mediated isothermal amplification for visual detection of *Vibrio parahaemolyticus* using gold nanoparticles. Microchim Acta 185:35–41
5. Li HH, Zhang YW, Luo YL, Sun XP (2011) Nano-C-60: a novel, effective, fluorescent sensing platform for biomolecular detection. Small 7:1562–1568
6. Wang XL, Niazi S, Yukun H, Sun WJ, Wu SJ, Duan N, Hun X, Wang ZP (2017) Homogeneous time-resolved FRET assay for the detection of Salmonella typhimurium using aptamer-modified $NaYF_4$:Ce/Tb nanoparticles and a fluorescent DNA label. Microchim Acta 184:4021–4027
7. Liu KY, Yan X, Mao BY, Wang S, Deng L (2016) Aptamer-based detection of *Salmonella enteritidis* using double signal amplification by Klenow fragment and dual fluorescence. Microchim Acta 183:643–649
8. Chinnappan R, AlAmer S, Eissa S, Rahamn AA, Abu Salah KM, Zourob M (2017) Fluorometric graphene oxide-based detection of *Salmonella enteritis* using a truncated DNA aptamer. Microchim Acta 185:61–69
9. He QZ, Luo HQ, Tang L, Liu J, Chen KK, Zhang QF, Ning Y (2017) Nanographite-based fluorescent biosensing of Salmonella

enteritidis by applying deoxyribonuclease-assisted recycling. Microchim Acta 184:3875–3882
10. Zhang Y, Zheng B, Zhu CF, Zhang X, Tan CL, Li H, Chen B, Yang J, Chen JZ, Huang Y, Wang LH, Zhang H (2015) Single-layer transition metal dichalcogenide nanosheet based nanosensors for rapid, sensitive, and multiplexed detection of DNA. Adv Mater 27:935–939
11. Yuan YX, Wu SF, Shu F, Liu ZH (2014) An MnO_2 nanosheet as a label-free nanoplatform for homogeneous biosensing. Chem Commun 50:1095–1097
12. Lin Y, Williams TV, Connell JW (2010) Soluble, exfoliated hexagonal boron nitride nanosheets. J Phys Chem Lett 1:277–283
13. Wang QB, Wang W, Lei JP, Xu N, Gao FL, Ju HX (2013) Fluorescence quenching of carbon nitride nanosheet through its interaction with DNA for versatile fluorescence sensing. Anal Chem 85:12182–12188
14. Lu CH, Yang HH, Zhu CL, Chen X, Chen GN (2009) A graphene platform for sensing biomolecules. Angew Chem Int Ed 48:4785–4787
15. Zhu CF, Zeng ZY, Li H, Li F, Fan CH, Zhang H (2013) Single-layer MoS_2-based nanoprobes for homogeneous detection of biomolecules. J Am Chem Soc 135:5998–6001
16. Li H, Eddaoudi M, O'Keeffe M, Yaghi OM (1999) Design and synthesis of an exceptionally stable and highly porous metal-organic framework. Nature 402:276–279
17. Zhou HC, Long JR, Yaghi OM (2012) Introduction to metal-organic frameworks. Chem Rev 112:673–674
18. Wu YF, Han JY, Xue P, Xu R, Kang YJ (2015) Nano metal-organic framework (NMOF)-based strategies for multiplexed microRNA detection in solution and living cancer cells. Nanoscale 7:1753–1759
19. Zhang HT, Zhang JW, Huang G, Du ZY, Jiang HL (2014) An amine-functionalized metal-organic framework as a sensing platform for DNA detection. Chem Commun 50:12069–12072
20. Liu TZ, Hu R, Zhang X, Zhang KL, Liu Y, Zhang XB, Bai RY, Li D, Yang YH (2016) Metal-organic framework nanomaterials as novel signal probes for electron transfer mediated ultrasensitive electrochemical immunoassay. Anal Chem 88:12516–12523
21. Shen WJ, Zhuo Y, Chai YQ, Yuan R (2015) Cu-based metal-organic frameworks as a catalyst to construct a ratiometric electrochemical aptasensor for sensitive lipopolysaccharide detection. Anal Chem 87:11345–11352
22. Xiong CY, Wang HJ, Liang WB, Yuan YL, Yuan R, Chai YQ (2015) Luminescence-functionalized metal-organic frameworks based on a ruthenium(II) complex: a signal amplification strategy for electrogenerated chemiluminescence immunosensors. Chem Eur J 21:9825–9832
23. Yang XL, Chen X, Hou GH, Guan RF, Shao R, Xie MH (2016) A multiresponsive metal-organic framework: direct chemiluminescence, photoluminescence, and dual tunable sensing applications. Adv Funct Mater 26:393–398
24. Wang B, Lv XL, Feng D, Xie LH, Zhang J, Li M, Xie Y, Li JR, Zhou HC (2016) Highly stable Zr(IV)-based metal-organic frameworks for the detection and removal of antibiotics and organic explosives in water. J Am Chem Soc 138:6204–6216
25. Zhu X, Zheng HY, Wei XF, Lin ZY, Guo LH, Qiu B, Chen GN (2013) Metal-organic framework (MOF): a novel sensing platform for biomolecules. Chem Commun 49:1276–1278
26. Hermosa C, Horrocks BR, Martinez JI, Liscio F, Gomez-Herrero J, Zamora F (2015) Mechanical and optical properties of ultralarge flakes of a metal-organic framework with molecular thickness. Chem Sci 6:2553–2558
27. Peng Y, Li YS, Ban YJ, Jin H, Jiao WM, Liu XL, Yang WS (2014) Metal-organic framework nanosheets as building blocks for molecular sieving membranes. Science 346:1356–1359
28. Xu H, Gao JK, Qian XF, Wang JP, He HJ, Cui YJ, Yang Y, Wang ZY, Qian GD (2016) Metal-organic framework nanosheets for fast-response and highly sensitive luminescent sensing of Fe^{3+}. J Mater Chem A 4:10900–10905
29. Junggeburth SC, Diehl L, Werner S, Duppel V, Sigle W, Lotsch BV (2013) Ultrathin 2D coordination polymer nanosheets by surfactant-mediated synthesis. J Am Chem Soc 135:6157–6164
30. Zhao MT, Wang YX, Ma QL, Huang Y, Zhang X, Ping JF, Zhang ZC, Lu QP, Yu YF, Xu H, Zhao YL, Zhang H (2015) Ultrathin 2D metal-organic framework nanosheets. Adv Mater 27:7372–7378
31. Zhao SL, Wang Y, Dong JC, He CT, Yin HJ, An PF, Zhao K, Zhang XF, Gao C, Zhang LJ, Lv JW, Wang JX, Zhang JQ, Khattak AM, Khan NA, Wei ZX, Zhang J, Liu SQ, Zhao HJ, Tang ZY (2016) Ultrathin metal-organic framework nanosheets for electrocatalytic oxygen evolution. Nat Energy 1:1–10
32. Lan LY, Chen DK, Yao Y, Peng XS, Wu J, Li YB, Ping JF, Ying YB (2018) Phase-dependent fluorescence quenching efficiency of MoS_2 nanosheets and their applications in multiplex target biosensing. ACS Appl Mater Interfaces 10:42009–42017
33. Wang Q, Wang W, Lei J, Xu N, Gao F, Ju H (2013) Fluorescence quenching of carbon nitride nanosheet through its interaction with DNA for versatile fluorescence sensing. Anal Chem 85:12182–12188
34. Wang WB, Liu LQ, Song SS, Xu LG, Kuang H, Zhu JP, Xu CL (2017) Identification and quantification of eight *Listeria monocytogene* serotypes from *Listeria spp.* using a gold nanoparticle-based lateral flow assay. Microchim Acta 184:715–724
35. Duan N, Wu SJ, Zhang HL, Zou Y, Wang ZP (2018) Fluorometric determination of *Vibrio parahaemolyticus* using an F0F1-ATPase-based aptamer and labeled chromatophores. Microchim Acta 185:304–309